

COCO-Occ: A Benchmark for Occluded Panoptic Segmentation and Image Understanding

1st Wenbo Wei

*Department of Computer Science
University of Warwick, UK
wenbo.wei@warwick.ac.uk*

2nd Jun Wang

*Department of Computer Science
University of Warwick, UK
jun.wang.3@warwick.ac.uk*

3rd Abhir Bhalerao

*Department of Computer Science
University of Warwick, UK
abhir.bhalerao@warwick.ac.uk*

Abstract—To help address the occlusion problem in panoptic segmentation and image understanding, this paper proposes a new large-scale dataset, COCO-Occ, which is derived from the COCO dataset by manually labelling the COCO images into three perceived occlusion levels. Using COCO-Occ, we systematically assess and quantify the impact of occlusion on panoptic segmentation on samples having different levels of occlusion. Comparative experiments with SOTA panoptic models demonstrate that the presence of occlusion significantly affects performance with higher occlusion levels resulting in notably poorer performance. Additionally, we propose a straightforward yet effective method as an initial attempt to leverage the occlusion annotation using contrastive learning to render a model that learns a more robust representation capturing different severities of occlusion. Experimental results demonstrate that the proposed approach boosts the performance of the baseline model and achieves SOTA performance on the proposed COCO-Occ dataset.

Index Terms—Occlusion, Contrastive Learning, Panoptic Segmentation.

I. INTRODUCTION

Owing to the release of large-scale datasets [1]–[6] and well-designed approaches, significant progress has been seen in the computer vision [7] and image understanding tasks. Nonetheless, the performance of some tasks, e.g., object detection [8]–[17], instance segmentation [18]–[23], and panoptic segmentation [24]–[32], still falls short of other tasks. The occlusion problem whereby some objects in the scene partially obscure others, is one of the key and most common issues that hampers the further performance improvement on various computer vision tasks such as object detection and segmentation. This is because algorithms struggle to perceive the occluded object and adequately extract its features. Figure 1 illustrates the occlusion problem for the panoptic segmentation task, where instances suffering from occlusion are wrongly predicted. To address this challenge, some studies have explored model architectures specially designed for handling occlusion in object detection [33] and instance segmentation [34]–[37]. For example, [33] introduces a Compositional Convolutional Neural Network (CompositionalNets), which enhances the robustness of deep convolutional neural networks for partial occlusion through integrating a differentiable compositional model. [34] generalizes CompositionalNets to

COCO-Occ database annotations and method code will be made available on acceptance of the paper.

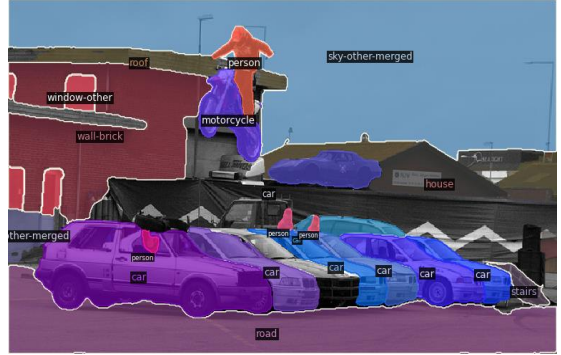


Fig. 1. Visualization of a prediction result by the Mask2Former [29] network. The third car from the left in the middle, the truck in the center, and the truck near the roof are not detected due to occlusion.

multi-object occlusion and proposes an Occlusion Reasoning Module (ORM) to post-hoc fix segmentation errors.

Although some performance gains have been achieved, these methods normally are developed as intuitive or rule-based due to the lack of large-scale occlusion annotation data, which hinders potential further improvements. Therefore, apart from the design of model architecture, datasets tailored for occlusion analysis are equally vital in research. [38] proposes a benchmark dataset, OVIS, for video instance segmentation [39] under severe occlusion. For each frame, they assign a unique occlusion level to the objects and define the Bounding-box Occlusion Rate (BOR) to qualify the occlusion level of the entire frame. [40] proposes MOSE, which partially inherits from OVIS, for video object segmentation in complex scenes. These datasets have promoted better methods for the video understanding task, but they are relatively small-scale and only covers a small part of commonly seen categories. In addition, few studies have explored the occlusion in 2D image scenes which is normally more challenging than 3D videos because of the absence of the time series information [24].

To fill this gap, we initiate our research by annotating occlusion levels of images from the commonly used image understanding benchmark, the COCO dataset [4]. Current methods for occlusion measurement, such as BOR, use the labelled image data to define an occlusion level as the Intersection over Union (IoU) calculated by bounding boxes of scene instances. However, in most cases, a bounding box does not fully enclose the entire object, leading to calculated

BOR values that fail to accurately represent the occlusion level. Moreover, BOR calculations heavily rely on the union area of the occluder and the occludee, neglecting the absolute area extent the object is occluded, which further reduces its utility in occlusion measurement. To this end, although labour intensive, we choose a direct approach and manually label the observed occlusion level of a scene, (low, mid, and high), resulting in a new dataset named COCO-Occ, as shown in Fig. 2. We then investigate the performance of recent SOTA methods [25]–[30] in understanding occluded images by exploring their performance in the challenging image understanding task, i.e., panoptic segmentation, on the proposed COCO-Occ dataset. Note although this work explores the proposed benchmark on a panoptic segmentation task, the proposed occlusion benchmark can be utilized to aid any image understanding tasks such as object detection and image recognition. Building on this, we further evaluate the newly trained Mask2Former [29] across different occlusion levels. The experimental results show that the performance decreases significantly as occlusion level increase from low to high, underscoring the challenge occlusion poses to SOTA panoptic segmentation methods.

As a first attempt to leverage the proposed occlusion annotations, here we also propose a contrastive learning-based method to improve the representation learning of panoptic segmentation. Specifically, we utilize a triplet loss to bring samples having the same occlusion level closer in the feature space, while pushing apart samples with differing levels. Experimental results demonstrate that the simple proposed method achieves the state-of-the-art performance on the COCO-Occ dataset. An ablation study further proves the effectiveness of the proposed method. In summary, our contributions are three-fold:

- We establish and release a large-scale dataset COCO-Occ, which aims to aid occluded image understanding tasks. This dataset is derived from the COCO dataset by manually annotating the observed occlusion level, resulting in 30,000 training images and 5,000 test images.
- We systematically investigate the influence of the occlusion level by exploring the performance of SOTA panoptic segmentation methods in understanding the occluded images on the proposed benchmark.
- We devise a method to leverage the proposed occlusion annotations using a contrastive learning to improve the representation learning for the panoptic segmentation task. The experimental results demonstrate the effectiveness of the proposed method.

II. METHOD

A. COCO-Occ Dataset

a) Dataset Annotation: We annotate the occlusion levels of the images by the following three steps. For all the selected images, we first overlay polygon masks according to the ground truth annotation using the COCO API, since polygon masks can more accurately delineate the area of objects

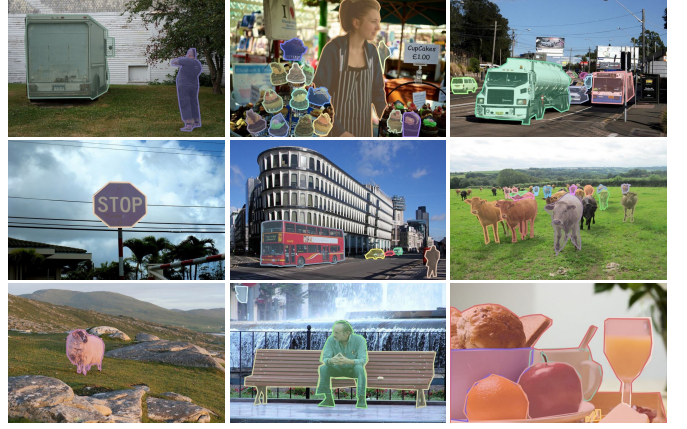


Fig. 2. Comparison of sample images with different occlusion levels from COCO-Occ dataset. All images are overlaid with ground truth annotations to better show the occlusion relationship. The left, mid, and right columns show sample images with low, mid, and high occlusion levels, respectively. It is important to mention that only annotated instances are taken into account for assessment of the occlusion level.

compared to bounding boxes. Then, we calculate the ratio of the occluded region to the entire occludee (including the occluded part), which is termed occlusion rate. However, we cannot obtain the area of the occluded region directly because the COCO annotation only provides masks for visible parts of the objects. To resolve this issue, we have referred to a theory suggesting that people can estimate the shape of the occluded part of an object based on its overall shape, category, or relationship with other objects [41]. Therefore, we opt to visually estimate the shape of the occluded region and thereby estimate the occlusion rate of the occludee. Finally, the highest occlusion rate is defined as the occlusion level of the image. Based on this criterion, we manually classify the images into three occlusion levels: low, mid, and high, corresponding to the occlusion rate of [0%], (0%, 50%), and (50%, 100%), respectively. If the occlusion rate is difficult to estimate, which is most often the case when determining the 50% threshold, we classify such images as having a mid occlusion level.

b) Dataset Statistic: The COCO-Occ dataset contains 35k images, with 30k training images selected from the original COCO training set (first 30k images) and 5k validation images which are the same as the original COCO validation set. For the training set, 12,081 images are annotated as high occlusion, 11,251 images as mid occlusion, and 6,668 images as low occlusion. For the validation set, 1,791 images are annotated as high occlusion, 2,075 images as mid occlusion, and 1,134 images as low occlusion. In addition, we separate the validation set into three subsets according to the occlusion level for further experimental validation of the models.

B. Contrastive Learning on Occlusion Level

Having the annotation of the occlusion level on hand, we aim to leverage this information to improve the model performance on occluded image understanding. The model is expected to recognize the different occlusion levels from different images, so as to learn a more robust feature representation. One simplest way is to form a classification

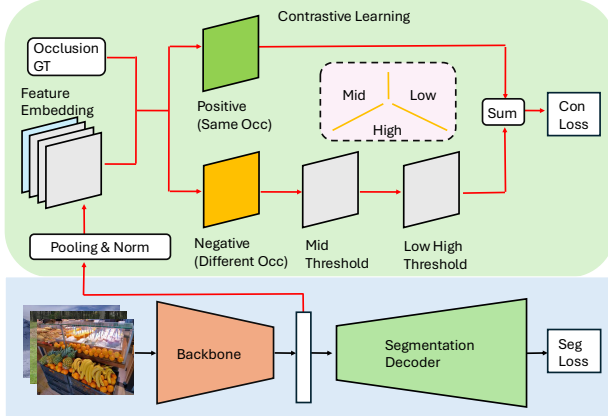


Fig. 3. The illustration of overall approach. The blue area below represents the schematic diagram of segmentation baseline, while the green area above illustrates our proposed contrastive learning-based method.

task based on the occlusion level. However, the classification requires samples from the same occlusion level to be strictly mapped into same latent space, ignoring the similarities among samples from different occlusion level as the occlusion is a high-level concept. To this end, we employ a relatively soft method, the contrastive learning method, on the high-level image understanding task, i.e, panoptic segmentation, to improve the feature representation learning on occlusion. Specifically, we regard image pairs with the same occlusion level as positive pairs and those with different occlusion levels as negative pairs. A distance-based triplet loss is adopted to implement contrastive learning which could tolerate some dissimilarities between negative pairs.

The overall architecture is illustrated in Figure 3. In particular, we first feed the feature maps from the final layer of the backbone through $Norm(AvgPool(X))$ to obtain the feature embeddings \tilde{z} . Then, we calculate the cosine similarity via function $Sim(\cdot)$ based on \tilde{z} between image samples within a batch and apply the triplet loss as shown in Equation 1 to enable contrastive learning. Where y_i denotes the occlusion label for i^{th} sample and τ is the margin.

$$L_{con} = \frac{1}{B^2} \sum_{i=1}^B \sum_{j:y_j^d=y_i^d}^B (1 - Sim(\tilde{z}_i, \tilde{z}_j)) + \sum_{j:y_j^d \neq y_i^d}^B \max(0, Sim(\tilde{z}_i, \tilde{z}_j) - \tau), \quad (1)$$

We observe that images between low and high occlusion levels show a more noticeable difference, while images between mid and low or high-level share more similarities in the occlusion space. Given this, we propose to set two margins to the low-high image pairs and other pairs respectively. Specifically, we set a strict threshold $\tau_{l,h}$ to push low-high image pairs closer and a higher threshold τ_m for other pairs to tolerate more dissimilarity.

Through the proposed contrastive learning can capture the occlusion difference from different samples, thereby learning a more discriminative and robust feature representation. The

TABLE I
SOTA PERFORMANCE ON DIFFERENT OCCLUSION LEVELS.

Method	Occlusion	PQ	PQ Th	PQ St	AP Th _{pan}	mIoU _{pan}
Panoptic FPN [25]	low	43.8	53.2	29.5	-	-
	mid	40.2	47.3	29.5	-	-
	high	34.5	39.0	27.7	-	-
Panoptic FCN [26]	low	46.9	56.1	33.3	-	-
	mid	41.9	48.2	32.5	-	-
	high	36.3	40.4	30.1	-	-
Panoptic DeepLab [27]	low	42.9	47.8	35.5	-	-
	mid	36.2	39.4	31.3	-	-
	high	30.3	31.0	29.2	-	-
MaskFormer [28]	low	52.6	58.8	43.3	-	-
	mid	48.0	53.9	39.1	-	-
	high	41.2	44.0	37.0	-	-
Mask2Former [29]	low	56.8	64.4	45.8	56.5	60.4
	mid	53.3	60.1	43.0	45.1	61.2
	high	46.7	51.3	39.7	35.8	58.1
Mask DINO [30]	low	56.6	63.1	47.0	56.4	58.0
	mid	53.7	60.6	43.4	47.2	59.7
	high	48.3	53.3	40.8	38.8	57.4

TABLE II
COMPARISON OF SOTA PANOPTIC SEGMENTATION METHODS ON THE COCO-OCC DATASET VIA RETRAINING ON COCO-OCC DATASET.

Model	PQ	PQ Th	PQ St	AP Th _{pan}	mIoU _{pan}
Panoptic FPN [25]	33.3	39.1	24.6	-	-
Panoptic-DeepLab [27]	27.5	28.9	25.3	-	-
Panoptic FCN [26]	33.0	37.7	26.0	-	-
Mask2Former [29]	41.5	45.3	35.6	30.6	54.4
Ours	41.8	45.3	36.4	30.8	54.3

model is jointly optimized by the proposed contrastive loss L_{con} and the panoptic segmentation loss L_{seg} . The final loss L_{fin} is shown in Equation 2 where λ is a hyper-parameter to balance the contribution between the segmentation loss the and occlusion-based contrastive learning.

$$L_{fin} = L_{seg} + \lambda L_{con} \quad (2)$$

III. EXPERIMENTS

We investigate how images with different occlusion levels affect the performance of SOTA panoptic segmentation method using the newly proposed COCO-Occ dataset. Apart from the standard panoptic segmentation metric PQ [24], we also report APTh_{pan} and mIoU_{pan} [29] for instance segmentation and semantic segmentation, respectively. Finally, we demonstrate the effectiveness of our proposed methods through ablation studies.

A. Implementation Details

For experiments investigating the influence of different occlusion levels, we conduct a validation experiment which loads the pretrained weights (trained on the entire COCO dataset) of recent SOTA panptic segmentation methods and tests their performance on the different validation subsets (occlusion level) of the proposed COCO-Occ using the official code and scripts. As for experiments verifying the effectiveness of our proposed method, we adopt the Mask2Former (with ResNet-50) as our baseline and train the model on the training set of our proposed COCO-Occ dataset. All the compared methods on this experiment are reimplemented on the COCO-Occ

TABLE III
COMPARISON ACROSS LOW, MID, AND HIGH OCCLUSION LEVELS FOR PROPOSED METHODS AND BASELINE VIA RETRAINING.

Occlusion	Model	PQ	PQ Th	PQ St	AP Th _{pan}	mIoU _{pan}
low	base	47.5	53.5	38.5	46.7	52.2
	con	48.1(+0.6)	53.1	40.8(+2.3)	46.4	52.7(+0.5)
mid	base	43.1	48.1	35.6	33.3	54.0
	con	43.2	47.9	36.1(+0.5)	33.7(+0.4)	54.0
high	base	35.7	38.2	32.0	24.8	50.7
	con	36.1(+0.4)	38.2	33.0(+1.0)	24.7	50.8

dataset using the official code. The input images are resized and cropped into 512×512 . λ in equation 2 is set to 1.0. The margins $\tau_{l,h}$ and τ_m are set to 0.4 and 0.6 respectively.

B. Experimental Results

Herein, we first benchmark the performance of the SOTA panoptic segmentation methods, including Panoptic FPN [25], Panoptic DeepLab [27], Panoptic FCN [26], Mask2Former [29] and Mask DINO [30], on the proposed COCO-Occ validation set. In particular, we report the results on different levels of occlusion (subsets), as shown in Table I. The results show a clear trend: As the level of occlusion increases from low to high, the performance metrics (PQ, PQTh, PQSt, and APTh_{pan}) experience a significant decline. This degradation highlights a critical limitation of current SOTA panoptic segmentation methods, which struggle to maintain accuracy and consistency in handling occlusion. Moreover, it also confirms the correctness of our manual annotation that reflects the level of occlusion of the image.

Then, we verify the effectiveness of our proposed method by retraining and testing the model on the COCO-Occ. We demonstrate the results of our proposed method and the baseline on all three levels of occlusion subsets of the validation set in Table III and compare our method with recent SOTA methods in Table II. As can be seen, the model equipped with the proposed contrastive learning shows substantial improvements at all levels of occlusion. Specifically, for low occlusion, PQ improves by 0.6, and PQSt sees a remarkable increase of 2.3, indicating a strong enhancement in the segmentation of ‘stuff’ classes. Similarly, under high occlusion, the method delivers a 0.4 improvement in PQ and a 1.0 increase in PQSt. All results demonstrate the effectiveness of our method compared to the baseline in a range of occlusion levels. Note that the panoptic segmentation is a challenging task, especially on the large-scale challenging dataset COCO, even a small improvement proves difficult. Moreover, our proposed method obtains the best overall performance over the previous SOTA methods. These results confirm our theory and demonstrate that the occlusion feature representation can assist in training and improve overall segmentation accuracy, especially in segmenting and labeling larger, less defined regions.

C. Ablation Study

In addition to the ablation study in Table III, we further conduct an ablation study to analyze the effectiveness of our method on the entire validation set. As shown in IV, after adding the proposed method, an improvements can be seen

TABLE IV
ABLATION STUDY ON THE PROPOSED METHOD.

Model τ	PQ	PQ Th	PQ St	AP Th _{pan}	mIoU _{pan}
Base	41.5	45.3	35.6	30.6	54.4
	41.8(+0.3)	45.3	36.4(+0.8)	30.8	54.3

TABLE V
IMPACT OF $\tau_{l,h}$ AND τ_m COMBINATIONS ON THE PERFORMANCE OF CONTRASTIVE LEARNING-BASED METHOD

$\tau_{l,h}$	τ_m	PQ	PQ Th	PQ St
0.3	0.4	41.3	45.0	35.8
0.3	0.6	41.2	44.9	35.6
0.3	0.8	41.4	45.2	35.7
0.4	0.6	41.8	45.3	36.4
0.4	0.7	41.3	45.1	35.7

on both the different occlusion subset and the entire validation set, especially PQSt improves by 0.8 on the entire validation set. This indicates that proposed contrastive learning method enables the model to learn a more occlusion-robust feature, thereby improving its overall performance.

Then, we investigate the influence of the margins in our proposed contrastive learning in Table V. Particularly, we first evaluate the threshold combination of $\tau_{l,h}$ and τ_m by keeping one threshold fixed while increasing the other. When the first threshold $\tau_{l,h}$ is fixed at 0.3, increasing the second threshold τ_m (from 0.4 to 0.8) shows minimal effect on overall performance. When $\tau_{l,h}$ is increased to 0.4, the combination of $\tau_{l,h} = 0.4$ and $\tau_m = 0.6$ achieves the highest PQ. However, under further increases of τ_m beyond 0.6, the overall performance starts to decline. This trend demonstrates that neglecting the influence of either threshold will result in a degradation of overall performance.

Our method is the initial attempt to utilize the occlusion annotations. We believe that a more significant improvement can be achieved when further advanced methods are proposed to take better advantage of our proposed dataset.

IV. CONCLUSION

In this work, we introduce COCO-Occ, a novel large-scale dataset designed to facilitate research on occlusion in panoptic segmentation and other image understanding tasks. The dataset, derived from the COCO dataset with manual occlusion annotations, provides a comprehensive benchmark with over 30,000 training and 5,000 test images categorized into three occlusion levels. Our experiments systematically evaluated the performance of SOTA panoptic segmentation methods on this dataset, revealing that occlusion, especially at higher levels, substantially degrades model performance. Additionally, we proposed a contrastive learning-based method to enhance model robustness in handling occlusion. Despite its simplicity, our approach yielded performance improvements over the baseline. This work not only highlights the significant impact of occlusion on panoptic segmentation task but offers a quantitative foundation for future research into more effective occlusion-aware methods.

REFERENCES

[1] J. Deng, W. Dong, R. Socher, L.-J. Li, K. Li, and L. Fei-Fei, "Imagenet: A large-scale hierarchical image database," in *2009 IEEE conference on computer vision and pattern recognition*. Ieee, 2009, pp. 248–255.

[2] B. Zhou, H. Zhao, X. Puig, S. Fidler, A. Barriuso, and A. Torralba, "Scene parsing through ade20k dataset," in *Proceedings of the IEEE conference on computer vision and pattern recognition*, 2017, pp. 633–641.

[3] M. Cordts, M. Omran, S. Ramos, T. Rehfeld, M. Enzweiler, R. Benenson, U. Franke, S. Roth, and B. Schiele, "The cityscapes dataset for semantic urban scene understanding," in *Proceedings of the IEEE conference on computer vision and pattern recognition*, 2016, pp. 3213–3223.

[4] T.-Y. Lin, M. Maire, S. Belongie, J. Hays, P. Perona, D. Ramanan, P. Dollár, and C. L. Zitnick, "Microsoft coco: Common objects in context," in *Computer Vision-ECCV 2014: 13th European Conference, Zurich, Switzerland, September 6-12, 2014, Proceedings, Part V 13*. Springer, 2014, pp. 740–755.

[5] G. Neuhold, T. Ollmann, S. Rota Bulo, and P. Kontschieder, "The mapillary vistas dataset for semantic understanding of street scenes," in *Proceedings of the IEEE international conference on computer vision*, 2017, pp. 4990–4999.

[6] A. Geiger, P. Lenz, and R. Urtasun, "Are we ready for autonomous driving? the kitti vision benchmark suite," in *2012 IEEE conference on computer vision and pattern recognition*. IEEE, 2012, pp. 3354–3361.

[7] R. Szeliski, *Computer vision: algorithms and applications*. Springer Nature, 2022.

[8] S. Ren, K. He, R. Girshick, and J. Sun, "Faster r-cnn: Towards real-time object detection with region proposal networks," *IEEE transactions on pattern analysis and machine intelligence*, vol. 39, no. 6, pp. 1137–1149, 2016.

[9] W. Liu, D. Anguelov, D. Erhan, C. Szegedy, S. Reed, C.-Y. Fu, and A. C. Berg, "Ssd: Single shot multibox detector," in *Computer Vision-ECCV 2016: 14th European Conference, Amsterdam, The Netherlands, October 11–14, 2016, Proceedings, Part I 14*. Springer, 2016, pp. 21–37.

[10] T.-Y. Ross and G. Dollár, "Focal loss for dense object detection," in *proceedings of the IEEE conference on computer vision and pattern recognition*, 2017, pp. 2980–2988.

[11] T.-Y. Lin, P. Dollár, R. Girshick, K. He, B. Hariharan, and S. Belongie, "Feature pyramid networks for object detection," in *Proceedings of the IEEE conference on computer vision and pattern recognition*, 2017, pp. 2117–2125.

[12] Z. Cai and N. Vasconcelos, "Cascade r-cnn: Delving into high quality object detection," in *Proceedings of the IEEE conference on computer vision and pattern recognition*, 2018, pp. 6154–6162.

[13] N. Carion, F. Massa, G. Synnaeve, N. Usunier, A. Kirillov, and S. Zagoruyko, "End-to-end object detection with transformers," in *European conference on computer vision*. Springer, 2020, pp. 213–229.

[14] X. Zhu, W. Su, L. Lu, B. Li, X. Wang, and J. Dai, "Deformable detr: Deformable transformers for end-to-end object detection," *arXiv preprint arXiv:2010.04159*, 2020.

[15] S. Liu, F. Li, H. Zhang, X. Yang, X. Qi, H. Su, J. Zhu, and L. Zhang, "Dab-detr: Dynamic anchor boxes are better queries for detr," *arXiv preprint arXiv:2201.12329*, 2022.

[16] H. Zhang, F. Li, S. Liu, L. Zhang, H. Su, J. Zhu, L. M. Ni, and H.-Y. Shum, "Dino: Detr with improved denoising anchor boxes for end-to-end object detection," *arXiv preprint arXiv:2203.03605*, 2022.

[17] A. Wang, H. Chen, L. Liu, K. Chen, Z. Lin, J. Han, and G. Ding, "Yolov10: Real-time end-to-end object detection," *arXiv preprint arXiv:2405.14458*, 2024.

[18] K. He, G. Gkioxari, P. Dollár, and R. Girshick, "Mask r-cnn," in *Proceedings of the IEEE international conference on computer vision*, 2017, pp. 2961–2969.

[19] S. Liu, L. Qi, H. Qin, J. Shi, and J. Jia, "Path aggregation network for instance segmentation," in *Proceedings of the IEEE conference on computer vision and pattern recognition*, 2018, pp. 8759–8768.

[20] D. Bolya, C. Zhou, F. Xiao, and Y. J. Lee, "Yolact: Real-time instance segmentation," in *Proceedings of the IEEE/CVF international conference on computer vision*, 2019, pp. 9157–9166.

[21] H. Chen, K. Sun, Z. Tian, C. Shen, Y. Huang, and Y. Yan, "Blendmask: Top-down meets bottom-up for instance segmentation," in *Proceedings of the IEEE/CVF conference on computer vision and pattern recognition*, 2020, pp. 8573–8581.

[22] X. Wang, R. Zhang, T. Kong, L. Li, and C. Shen, "Solov2: Dynamic and fast instance segmentation," *Advances in Neural information processing systems*, vol. 33, pp. 17721–17732, 2020.

[23] Y. Lee and J. Park, "Centermask: Real-time anchor-free instance segmentation," in *Proceedings of the IEEE/CVF conference on computer vision and pattern recognition*, 2020, pp. 13906–13915.

[24] A. Kirillov, K. He, R. Girshick, C. Rother, and P. Dollár, "Panoptic segmentation," in *Proceedings of the IEEE/CVF conference on computer vision and pattern recognition*, 2019, pp. 9404–9413.

[25] A. Kirillov, R. Girshick, K. He, and P. Dollár, "Panoptic feature pyramid networks," in *Proceedings of the IEEE/CVF conference on computer vision and pattern recognition*, 2019, pp. 6399–6408.

[26] Y. Li, H. Zhao, X. Qi, L. Wang, Z. Li, J. Sun, and J. Jia, "Fully convolutional networks for panoptic segmentation," in *Proceedings of the IEEE/CVF conference on computer vision and pattern recognition*, 2021, pp. 214–223.

[27] B. Cheng, M. D. Collins, Y. Zhu, T. Liu, T. S. Huang, H. Adam, and L.-C. Chen, "Panoptic-deeplab: A simple, strong, and fast baseline for bottom-up panoptic segmentation," in *Proceedings of the IEEE/CVF conference on computer vision and pattern recognition*, 2020, pp. 12475–12485.

[28] B. Cheng, A. Schwing, and A. Kirillov, "Per-pixel classification is not all you need for semantic segmentation," *Advances in neural information processing systems*, vol. 34, pp. 17864–17875, 2021.

[29] B. Cheng, I. Misra, A. G. Schwing, A. Kirillov, and R. Girdhar, "Masked-attention mask transformer for universal image segmentation," in *Proceedings of the IEEE/CVF conference on computer vision and pattern recognition*, 2022, pp. 1290–1299.

[30] F. Li, H. Zhang, H. Xu, S. Liu, L. Zhang, L. M. Ni, and H.-Y. Shum, "Mask dino: Towards a unified transformer-based framework for object detection and segmentation," in *Proceedings of the IEEE/CVF Conference on Computer Vision and Pattern Recognition*, 2023, pp. 3041–3050.

[31] Z. Li, W. Wang, E. Xie, Z. Yu, A. Anandkumar, J. M. Alvarez, P. Luo, and T. Lu, "Panoptic segformer: Delving deeper into panoptic segmentation with transformers," in *Proceedings of the IEEE/CVF conference on computer vision and pattern recognition*, 2022, pp. 1280–1289.

[32] J. Jain, J. Li, M. T. Chiu, A. Hassani, N. Orlov, and H. Shi, "Oneformer: One transformer to rule universal image segmentation," in *Proceedings of the IEEE/CVF Conference on Computer Vision and Pattern Recognition*, 2023, pp. 2989–2998.

[33] A. Kortylewski, Q. Liu, A. Wang, Y. Sun, and A. Yuille, "Compositional convolutional neural networks: A robust and interpretable model for object recognition under occlusion," *International Journal of Computer Vision*, vol. 129, pp. 736–760, 2021.

[34] X. Yuan, A. Kortylewski, Y. Sun, and A. Yuille, "Robust instance segmentation through reasoning about multi-object occlusion," in *Proceedings of the IEEE/CVF Conference on Computer Vision and Pattern Recognition*, 2021, pp. 11141–11150.

[35] Y.-T. Chen, X. Liu, and M.-H. Yang, "Multi-instance object segmentation with occlusion handling," in *Proceedings of the IEEE Conference on Computer Vision and Pattern Recognition*, 2015, pp. 3470–3478.

[36] G. Zhan, W. Xie, and A. Zisserman, "A tri-layer plugin to improve occluded detection," *arXiv preprint arXiv:2210.10046*, 2022.

[37] L. Ke, Y.-W. Tai, and C.-K. Tang, "Deep occlusion-aware instance segmentation with overlapping bilayers," in *Proceedings of the IEEE/CVF conference on computer vision and pattern recognition*, 2021, pp. 4019–4028.

[38] J. Qi, Y. Gao, Y. Hu, X. Wang, X. Liu, X. Bai, S. Belongie, A. Yuille, P. H. Torr, and S. Bai, "Occluded video instance segmentation: A benchmark," *International Journal of Computer Vision*, vol. 130, no. 8, pp. 2022–2039, 2022.

[39] L. Yang, Y. Fan, and N. Xu, "Video instance segmentation," in *Proceedings of the IEEE/CVF International Conference on Computer Vision*, 2019, pp. 5188–5197.

[40] H. Ding, C. Liu, S. He, X. Jiang, P. H. Torr, and S. Bai, "Mose: A new dataset for video object segmentation in complex scenes," *arXiv preprint arXiv:2302.01872*, 2023.

[41] S. E. Palmer, *Vision science: Photons to phenomenology*. MIT press, 1999.